

Comparative study on the lamellar crystal structure of high and low density polyethylenes

Romeu A. Pereira^{1,*}, Eloisa B. Mano², Marcos L. Dias², Elen B. Acordi²

¹ Centro Brasileiro de Pesquisas Físicas – CNPq, Rua Xavier Sigaud, 150-22290-180 Rio de Janeiro, RJ – Brazil

² Instituto de Macromoléculas Professora Eloisa Mano, Universidade Federal do Rio de Janeiro, C.P. 68525, 21945-970 Rio de Janeiro, RJ – Brazil

Received: 22 January 1997/Revised version: 26 March 1997/Accepted: 31 March 1997

Summary

A comparative study was undertaken on well characterized HDPE and LDPE samples in order to obtain a better understanding of the morphology of the crystalline phase. Thickness of the lamellae was determined by WAXS. The melting points were calculated by empirical and Gibbs-Thomson equations, considering either folded or extended chains, and compared to DSC data. The results confirm that in HDPE the chains are folded, the segment between folds containing about 100 carbon atoms, while in LDPE, the chains are extended, with segments of about 73 carbon atoms in the crystalline core, linked to the paracrystalline layer and amorphous zones, which contain long folds and chain ends, as proposed in the 3-phase model by Vile *et al.*

INTRODUCTION

Polyethylene is one of the most investigated among all the polymers. Commercially, several types of polyethylenes are available with a variable range of crystallinity and density values, determined by the amount and size of chain branches. Linear polymers with no branches as in HDPE to polymers having short and long branches as in LDPE are industrially produced. As previously demonstrated, the short branches in LDPE are mainly n-butyl, but ethyl and possibly n-amyl and n-hexyl groups in smaller proportions are also formed by intramolecular "backbiting" (1). The long branches contain many tens or hundreds of carbon atoms and are formed by intermolecular chain transfer (1-4). The presence of these branches determines the crystallization degree and transition temperatures and affects the crystallographic parameters such as unit cell dimensions, setting angle and crystallite size (5).

Like HDPE, LDPE may crystallize from the melt as aggregates of lamellae organized in a spherulitic form. As very well documented in the literature, in the HDPE

* Corresponding author

crystallized from melt or solution these lamellae are constituted by folded chains in which adjacent reentries of the chain predominate (6,7). The non-crystalline part of the polyethylenes is composed by entangled chains and surface fold defects produced by non-adjacent reentries, cilia and tie molecules (5). It is also reported that in the crystallization of HDPE, under proper conditions, extended-chain crystals may also be present (8). Empirical correlations between the melting temperature of the polymer and molecular length of the extended chain as well as folded chain lamellae have been proposed. In terms of crystal structure, when compared to the linear polymer the branched polymer shows higher cell parameter, smaller crystallite size, lower crystallinity index and larger crystalline disorder (8-11).

No report was found in the literature, correlating crystallographic and thermal analysis data with the type of lamellae in polyethylenes. This paper presents the results of a comparative wide angle X-ray scattering (WAXS) and differential scanning calorimetry (DSC) study on LDPE and HDPE, showing the correlation between lamellar length and crystal melting temperature in these polymers.

EXPERIMENTAL

Samples

Two commercial polyethylene samples were used: HDPE BT003 (Polialden), $M_w = 84800$, $M_w/M_n = 13$, MFI = 0.3 g/10 min, density = 0.95 g/cm³, $T_m = 129^\circ\text{C}$; and LPDE 680/59 (Poliiolefinas), $M_w = 86900$, $M_w/M_n = 5$, MFI = 2.7g/ 10 min, $T_m = 108^\circ\text{C}$, density = 0.92g/cm³. Samples for WAXS were taken from a quenched film, compression molded at 188°C for 5 minutes.

WAXS measurements

WAXS measurements were performed in a standard Rich. Seifert Freiberg Präzisionsmechanik GmbH diffractometer operating with CoK α radiation ($\lambda = 1.7902\text{\AA}$) at room temperature in 40kV and 30mA and equipped with a graphite monochromator in the scattered beam, step-by-step mode, θ - 2θ Bragg-Brentano focusing condition with 0.25° divergent slit in the primary beam and 0.05° in the scattered beam. The interval from 5° to 115° in 2θ was used.

Sample crystal parameters were obtained refining the WAXS patterns by using the Rietveld Analysis Program DBWS-9411 (1994 version), and atomic position parameters, from Kavesh and Schultz model of polyethylene unit cell (12). Background radiation parameters and the crystalline part of the patterns were deconvoluted from the amorphous region.

The setting angle (ϕ) as defined by Bunn (13) is that subtended by the chain to the b -axis of the crystal unit cell and has been calculated using the refined structure parameters from Rietveld analysis. The crystallite size and paracrystalline disorder were calculated according to Hosemann's method (14).

DSC measurements

DSC analyses were carried out by a Perkin Elmer DSC-7 instrument under a nitrogen atmosphere. Annealing procedure consisted in cooling the sample at 50°C/min from 150°C to the desired temperature and maintaining it for one hour before cooling to room temperature. Thermal curves were recorded at 10°C/min.

RESULTS AND DISCUSSION

Wide Angle X-ray Scattering

The WAXS patterns of polyethylenes are dominated by two strong Bragg reflections from (110) and (200) planes, with many peaks of lower intensities. Figure 1 shows the θ - 2θ scan pattern of HDPE at room temperature, with the inset showing the magnification of the part which contains the (hkl) plane reflections at higher 2θ angles. The values for cell dimensions such as setting angles of the chain (φ), full-width at half-maximum (FWHM), crystallite size (L), the liquid-like disorder parameter (α), paracrystalline distortion (g), and unit cell density (ρ_c) computed from the refinement of the pattern data are listed in Table 1.

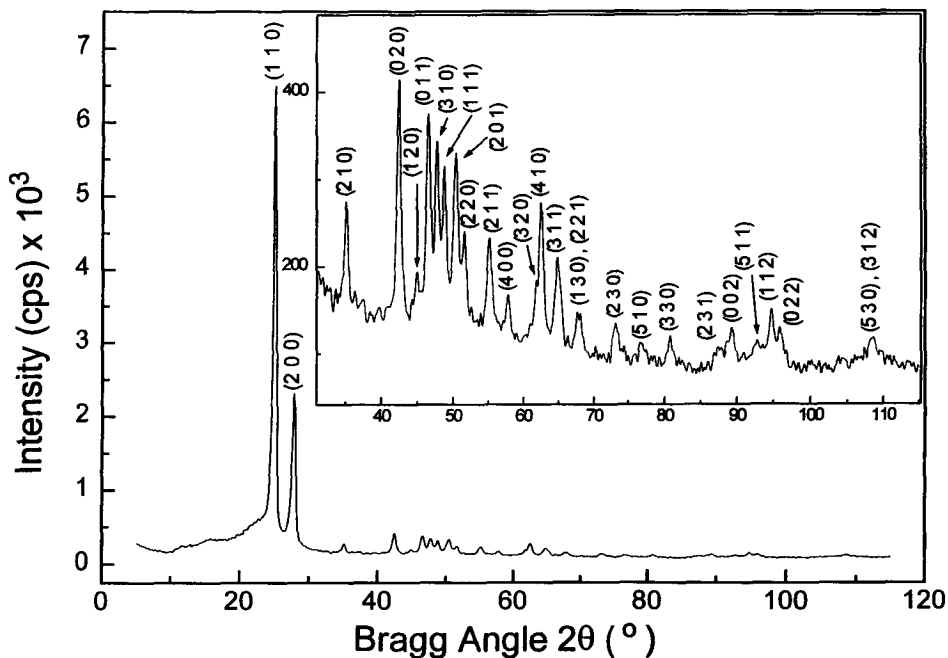


Figure 1. WAXS of HDPE at 23°C.

The unit cell dimensions obtained are in agreement with the reported values for orthorhombic polyethylene (11-15) and show that the presence of defects in the crystal lattice such as branches, increases the setting angle and cell parameter in the LDPE crystal lattice. The relative netplane fluctuation in both HDPE and LPDE is lower in the [001] direction, which is coincident with the chain axis in the crystal, and are higher in the [110] direction, with the largest crystallite size. The line width reflections for LDPE are

Table 1. Crystallographic data for HDPE and LDPE films at 23°C.

Sample	(hkl)	d (Å)	FWHM (°)	L (Å)	g (%)
HDPE	(110)	4.1111	0.4149	264.4	2.17
	(200)	3.7080	0.4366	252.7	2.11
	(020)	2.4707	0.5706	201.3	1.93
	(002)	1.2732	1.1910	126.4	1.75
Unit cell parameters					
		$\varphi=(45.8\pm 1)^\circ$	$\alpha = 0.17$	$\rho_c=0.9998(18) \text{ g/cm}^3$	
		$ \vec{a} =7.4087(18) \text{ \AA}$	$ \vec{b} =4.9372(9) \text{ \AA}$	$ \vec{c} =2.5469(5) \text{ \AA}$	

LDPE	(110)	4.1437	0.5983	181.9	2.50
	(200)	3.7407	0.6250	175.1	2.42
	(020)	2.4883	0.7936	143.5	2.18
	(002)	1.2778	1.6046	92.8	1.94
Unit cell parameters					
		$\varphi=(48.2\pm 1)^\circ$	$\alpha = 0.18$	$\rho_c=0.9805(26) \text{ g/cm}^3$	
		$ \vec{a} =7.4754(25) \text{ \AA}$	$ \vec{b} =4.9727(14) \text{ \AA}$	$ \vec{c} =2.5554(9) \text{ \AA}$	

broader than those of the corresponding HDPE. These differences are due not only to the lower crystal thickness and larger crystalline distortions, but also to additional distortions attributed to lattice strain in the chain direction [001], and the existence of a transition layer where the side branches are accommodated, generating stresses at the lamellar surface (16).

The melting temperature of a folded-chain lamellae with thickness L_c is given by the so-called Gibbs–Thomson equation (17):

$$T_m = T_m^0 \left(1 - \frac{2\sigma_e}{\Delta H_m^0 \rho_c L_c} \right) \quad \text{eq. (1)}$$

where T_m^0 is the equilibrium melting temperature, ρ_c the crystalline density, and σ_e the surface specific enthalpy. Brown and Eby (18) showed that for HDPE folded-chain lamellae the following empirical equation holds:

$$T_m = T_m^0 \left(\frac{n}{n + 3.1} \right) \quad \text{eq. (2)}$$

where n is the number of methylene units in the chain segments between folds. Similarly, for extended-chain lamellae as well as for the melting point of paraffins, the Broadhurst equation (9) holds:

$$T_m = T_m^0 \left(\frac{n - 1.5}{n + 5.0} \right) \quad \text{eq. (3)}$$

In order to investigate the type of morphology existing in the interface crystalline lamella/disordered phase, we applied eq. (1), (2) and (3) to calculate T_m for the samples under investigation. The lower and upper values reported in the literature for T_m^0 (9,19) were taken as standard values and are listed in Table 2, where $n = \frac{L_{1001}}{|\bar{c}|/2}$ is the number of carbon atoms in the chain segments of the crystalline core of the lamella.

Table 2. T_m values determined by DSC and calculated from WAXS data for HDPE and LDPE.

Amostra	$L_{[1001]}$ (Å)	n	$T_m(^{\circ}\text{C})^a$		$T_m(^{\circ}\text{C})^b$		$T_m(^{\circ}\text{C})^c$	$T_m(^{\circ}\text{C})_d$
			$T_m^o(^{\circ}\text{C})$ 141.4	$T_m^o(^{\circ}\text{C})$ 145.8	$T_m^o(^{\circ}\text{C})$ 141.4	$T_m^o(^{\circ}\text{C})$ 145.8	$T_m^o(^{\circ}\text{C})$ 145.8	
HDPE	126.4	100	128.9	133.2	115.5	119.9	127.8	129.0
LDPE	92.4	73	124.5	128.9	107.0	113.3	—	108.0

^a Calculated by eq (2)

^b Calculated by eq (3)

^c Calculated by eq (1) and data from ref. (20)

^d DSC measurement from ref. (21)

For the HDPE sample, the value obtained by DSC is in agreement with that calculated from eq. (2) using $T_m^0 = 141.4^\circ\text{C}$, and from eq. (1) adopting $T_m^0 = 145.8^\circ\text{C}$. Both equations refer to lamellae with folds on the transition surface between crystalline and amorphous phases. For the LDPE sample, the experimental T_m value agrees only with that calculated by eq. (3) using $T_m^0 = 141.4^\circ\text{C}$, suggesting that the crystalline lamellae surface did not contain chain folds, i.e., the melting proceeds as in the case of extended-chain crystals. This result is in close agreement with the model proposed by Vile and coworkers for LDPE (1), in which 3 phases are present: a crystalline core, a paracrystalline layer and an amorphous phase. The crystalline core is sandwiched between two paracrystalline layers. According to this model the lamellae core is crystalline, highly ordered, composed of linear, unbranched segments of several chains, organized as extended-chain zones. These chains are scarcely branched, mostly amyl or longer segments, transition zones (paracrystalline layers). These chains are more branched parts of the carbon chain and end groups, remaining as a liquid-like amorphous phase, in which the longer segment branches may reenter the paracrystalline or crystalline lamella regions.

Differential Scanning Calorimetry

Figure 2 presents DSC curves of LDPE. Curve 2a shows the peak of the sample two years after the molding. The LDPE sample showed a $T_m = 113.5^\circ\text{C}$ which is higher than that obtained just after sample preparation ($T_m = 108^\circ\text{C}$). Before the run which generated Curve 2b, the sample was cooled at $10^\circ\text{C}/\text{min}$ from the melt (160°C) to 90°C and kept at this temperature for one hour. Curve 2b shows that annealing had a small effect on the higher melting point crystals (maximum at 112°C). However, the curve shows bimodality, indicating that a second family of lamellae was affected by the annealing. Curve 2c shows another annealing treatment. The sample was cooled at $50^\circ\text{C}/\text{min}$ from 160°C to 100°C and maintained at this temperature for one hour. It is also multimodal, indicating two well-defined families of crystal lamellae: a thicker one ($T_m = 111^\circ\text{C}$) and another, melting at about 103°C .

The annealing behavior observed by us for LDPE had been previously reported by Rueda et al. (22). These authors interpreted the low temperature peaks developed by annealing as a low molecular-weight component which forms a thinner lamellae, although, even after solvent extraction, the presence of lower melting was observed by DSC traces.

Assuming the 3-phase model and in view of our results, we suggest that the low and high temperature peaks may be due to the paracrystalline region and crystalline core, respectively. If the crystalline core is constituted by extended-chain lamellae in which the surface, i.e., the interface between crystalline core and paracrystalline layers, is determined only by the presence of branch points, it is more plausible that faster cooling would cause insignificant changes in the lamella thickness. Thus, for this type of lamellae, the equilibrium temperature seems to be a function of the number of chain branches, for each macrochain. The interface between the paracrystalline layer and the amorphous phase in LDPE behaves as the interface of folded chain lamella and the amorphous phase in HDPE. During annealing, rearrangements of long and non-adjacent folds and molecular segments in the amorphous phase increase the thickness of the paracrystalline layers.

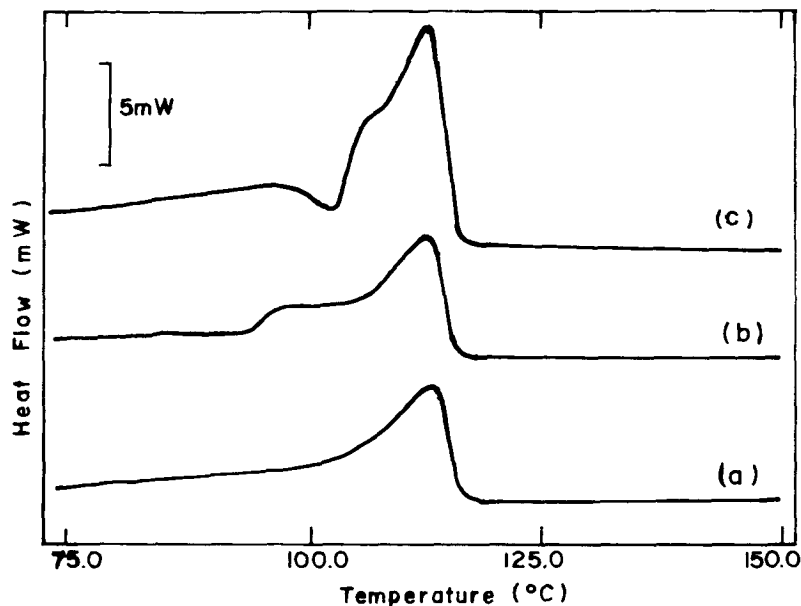


Figure 2. DSC Curves of LDPE: (a) after 2 years at room temperature without annealing; (b) annealed at 90°C for 1h after cooling at 10°C/min from 160°C; (c) annealed at 50°C/min at 100°C for 1h after cooling from 160°C.

CONCLUSIONS

WAXS and DSC were applied to characterize the lamellar structure of HDPE and LDPE samples. The experimental results, in addition to theoretical and empirical equations, indicate two families of ordered structures in LDPE. The more ordered one is due to extended chains with dimensions controlled by the amount and distribution of branches in the polymer chain. The second, less ordered structure, is due to the paracrystalline zone.

Acknowledgment

The authors are indebted to Mr. Sérgio C. Albuquerque Filho for his efficient help in the preparation of this manuscript. This work was supported by the Brazilian agencies *Conselho Nacional de Desenvolvimento Científico e Tecnológico (CNPq)* and *Coordenação do Aperfeiçoamento de Pessoal de Nível Superior (CAPES)*.

REFERENCES

1. Vile J, Hendra PJ, Willis HA, Cudby MEA, Bunn A (1984) *Polymer* 25: 1173
2. Shirayama K, Okada T, Kita SI (1965) *J Polym Sci A3*: 907
3. Randall JC (1973) *J Polym Sci Polym Phys Ed* 11: 275
4. Bovey FA, Schilling FC, McCrackin FL, Wagner HL (1976) *Macromolecules* 9: 76
5. Keith HD, Padden Jr FJ (1963) *J Appl Phys* 34: 2409
6. Spells SJ, Sadler DM, Keller A (1980) *Polymer* 21: 1121
7. Jing X, Krimm S (1982) *J Polym Sci Polym Lett Ed* 21: 123
8. Anderson FR (1964) *J Appl Phys* 35: 64
9. Broadhurst MG (1962) *J Chem Phys* 36: 2578
10. Davis GT, Eby RK, Martin GM (1968) *J Appl Phys* 39: 4973
11. Davis GT, Eby RK, Colson JP (1970) *J Appl Phys* 41: 4316
12. Kavesh S, Schultz JM (1970) *J Polym Sci A2* 8: 243
13. Bunn CW (1939) *Trans Faraday Soc* 35: 482
14. Hosemann R, Vogel W, Weick D, Baltá-Calleja FJ (1981) *Acta Cryst A37* : 85
15. Cole EA, Holmes DR (1960) *J Polym Sci* 46: 245
16. Hendra PJ, Passingham C (1991) *Eur Polym J* 27: 127
17. Hoffman JD, Weeks JJ (1961) *J Res Natl Bur Std* 66A: 13
18. Brown RG, Eby RK (1964) *J Appl Phys* 35: 1156
19. Wunderlich B (1980) in *Macromolecular Physics*, Chapter 8, Vol 3, Academic Press, New York
20. Mathot VB (1984) *Polymer* 25 : 579
21. Pacheco BAVE (1993) Thesis, Institute of Macromolecules, Federal University of Rio de Janeiro
22. Rueda DR, Martinez-Salazar J, Baltá-Calleja FJ (1984) *J Polym Sci* 22 : 1811